

PAPER • OPEN ACCESS

## Application of probabilistic modelling for the uncertainty evaluation of alignment measurements of large accelerator magnets assemblies

To cite this article: I Doytchinov *et al* 2018 *Meas. Sci. Technol.* **29** 054001

View the [article online](#) for updates and enhancements.

You may also like

- [Alignment Offset Analyzer against Wafer-Induced Shift](#)  
Hideki Ina, Takahiro Matsumoto and Koichi Sentoku
- [Analyses of Alignment Measurement Error](#)  
Ayako Sugaya
- [Efficiency of analytical and sampling-based uncertainty propagation in intensity-modulated proton therapy](#)  
N Wahl, P Hennig, H P Wieser et al.

# Application of probabilistic modelling for the uncertainty evaluation of alignment measurements of large accelerator magnets assemblies

I Doitchinov<sup>1,2</sup>, X Tonnellier<sup>2</sup>, P Shore<sup>2,3</sup>, B Nicquevert<sup>1</sup>, M Modena<sup>1</sup> and H Mainaud Durand<sup>1</sup>

<sup>1</sup> European Council for Nuclear Research—CERN, Route de Meyrin 385, 1217 Meyrin, Switzerland

<sup>2</sup> Cranfield University Precision Engineering Institute, College Rd, Cranfield, MK43 0AL, United Kingdom

<sup>3</sup> National Physical Laboratory—NPL, Hampton Road, Teddington, TW11 0LW, United Kingdom

E-mail: [Jordan.Doitchinov@gmail.com](mailto:Jordan.Doitchinov@gmail.com)

Received 5 December 2017, revised 15 January 2018

Accepted for publication 2 February 2018

Published 15 March 2018



## Abstract

Micrometric assembly and alignment requirements for future particle accelerators, and especially large assemblies, create the need for accurate uncertainty budgeting of alignment measurements. Measurements and uncertainties have to be accurately stated and traceable, to international standards, for metre-long sized assemblies, in the range of tens of  $\mu\text{m}$ . Indeed, these hundreds of assemblies will be produced and measured by several suppliers around the world, and will have to be integrated into a single machine. As part of the PACMAN project at CERN, we proposed and studied a practical application of probabilistic modelling of task-specific alignment uncertainty by applying a simulation by constraints calibration method. Using this method, we calibrated our measurement model using available data from ISO standardised tests (10360 series) for the metrology equipment. We combined this model with reference measurements and analysis of the measured data to quantify the actual specific uncertainty of each alignment measurement procedure. Our methodology was successfully validated against a calibrated and traceable 3D artefact as part of an international inter-laboratory study. The validated models were used to study the expected alignment uncertainty and important sensitivity factors in measuring the shortest and longest of the compact linear collider study assemblies, 0.54 m and 2.1 m respectively. In both cases, the laboratory alignment uncertainty was within the targeted uncertainty budget of 12  $\mu\text{m}$  (68% confidence level). It was found that the remaining uncertainty budget for any additional alignment error compensations, such as the thermal drift error due to variation in machine operation heat load conditions, must be within 8.9  $\mu\text{m}$  and 9.8  $\mu\text{m}$  (68% confidence level) respectively.

Keywords: precision measurement, alignment, uncertainty modelling, CMM, magnet alignment

(Some figures may appear in colour only in the online journal)



Original content from this work may be used under the terms of the [Creative Commons Attribution 3.0 licence](https://creativecommons.org/licenses/by/3.0/). Any further distribution of this work must maintain attribution to the author(s) and the title of the work, journal citation and DOI.

## 1. Introduction

The requirements of alignment and pre-alignment in the compact linear collider study (CLIC) [1] for the future 40 km range

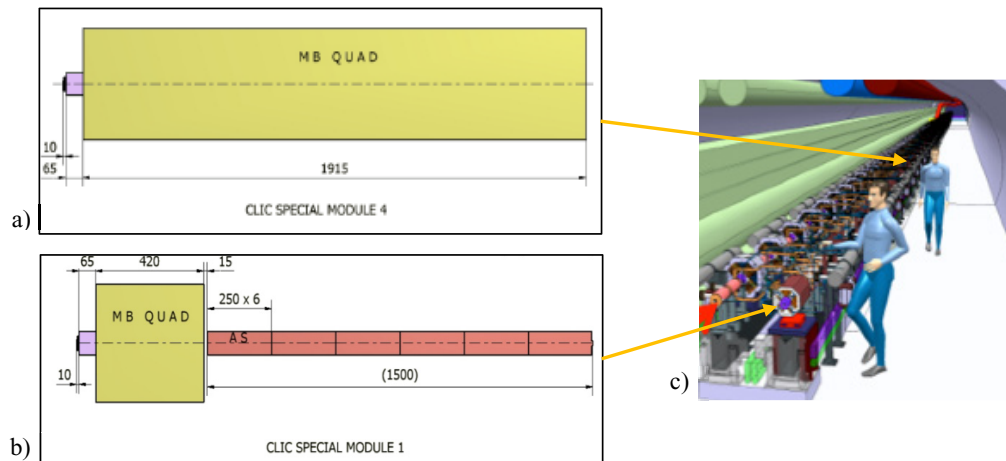


**Figure 1.** (a) CLIC special module 4 or type 4 assembly (longest magnet). (b) CLIC special module 1 or type 1 assembly (shortest magnet). (c) Sequential installation and alignment of magnets via high-precision positioning systems within the machine tunnel.

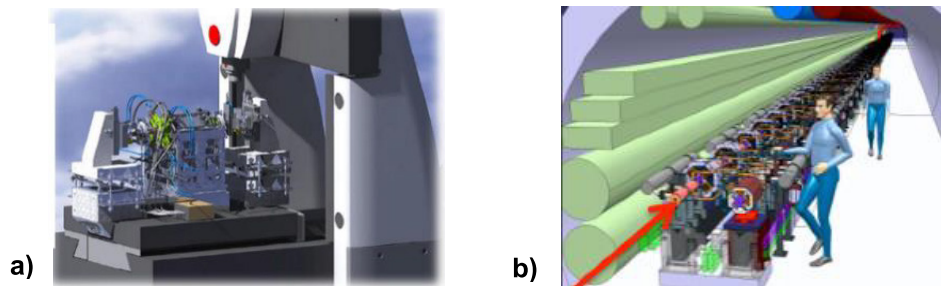


**Figure 2.** (a) Pre-alignment metrology completed at CMM environment. (b) Alignment of components in the tunnel with nano-positioning actuators using pre-alignment metrology data.

linear accelerator will be highly demanding. CLIC will host more than 20 000 modules up to two metres in length, integrated into series. There are five families of module assemblies, each containing either accelerating structures (AS) to accelerate particles or main beam quadrupole magnets (MB QUADS) to focus particles, or both. Four of the five module types have MB QUADS of varying lengths. The assembly module type with the longest magnet (1915 mm) is the ‘CLIC special module 4’, or type 4, shown in figure 1(a), of which 1472 units must be assembled and aligned [1]. The assembly with the shortest magnet (420 mm) is shown in figure 1(b). This is the ‘CLIC special module 1’, or type 1 magnet assembly, of which 308 units must be assembled and aligned within the accelerator.

The alignment of each magnetic or electrical axis of CLIC components should be within a  $14\ \mu\text{m}$ – $17\ \mu\text{m}$  diameter cylindrical tolerance zone with respect to a global reference at a  $1\sigma$  confidence interval. The global alignment reference for these 2 m modules is provided by a series of overlapping stretched wires, each of 200 m length. These requirements lead to a target uncertainty of alignment measurement of  $12\ \mu\text{m}$  at  $1\sigma$  for assembly sizes varying from 0.6 m to more than 2 m in length. The difference between the targeted measurement uncertainty ( $12\ \mu\text{m}$  at  $1\sigma$ ) and CLIC alignment tolerance zone ( $14\ \mu\text{m}$ – $17\ \mu\text{m}$  at  $1\sigma$ ) is due to the extra budget required for the magnet-to-magnet alignment reference system based on capacitive wire positioning sensors (WPS). The WPS system links each assembly reference frame with the global tunnel reference currently defined as a stretched thin wire [2]. These

demanding requirements have to be achieved for a large number of modules, which will be assembled and measured by several companies and laboratories located in CERN member states around the world.

A suitable method by which to achieve this targeted uncertainty was studied as part of the ‘particle accelerator components’ metrology and alignment to the nanometre-scale’ (PACMAN) program [3] run at CERN. In this method, magnetic and electrical axis metrology and geometrical surveys were performed simultaneously within the measurement environment of a coordinate measurement machine (CMM) such as the Leitz PMM-C Infinity (figure 2(a)) [4]. These measurements were performed in a class 1 metrology thermal environment with a temperature variation of  $\pm 0.1\ ^\circ\text{C}$  (ISO 14644-1). The minimum test current within the coils (required for magnetic measurements) was used, with no water-cooling, so as to minimise any possible thermal perturbations of the measurement environment. During the accelerator operation, accelerator structures would be thermally loaded from the full magnet power, water cooling systems and airflow within the machine tunnel. This would create large thermal gradients within the structures, with tens of Celsius degrees of variance from the  $20\ ^\circ\text{C}$  alignment laboratory temperature. Thus, compensation of CMM alignment measurements for drifts in both magnetic axis and spherical reference targets (fiducials) will be required figure 2(b).

Prior to the current study (part of the PACMAN project at CERN), the possibility of achieving traceable (to the Standard

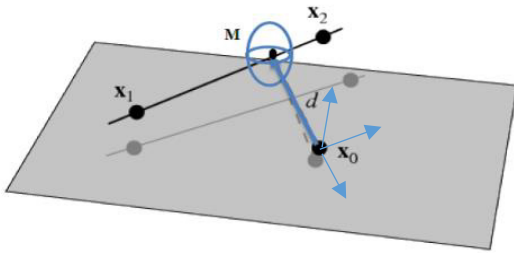


**Figure 3.** Pre-alignment metrology defined as knowledge of the magnetic axis location ( $X_1$ - $X_2$ ) with respect to assembly coordinate frame  $X_0$ .

International [5] realisation of the unit metre) micrometric alignment for metre-sized assemblies at an international and large industrial scale was not evaluated. Current work showed that such targets are achievable. It quantifies the available tolerance left over for any thermal error corrections required for post-metrology drift effects. In this work, the target uncertainty is defined by an ellipsoid describing the  $1\sigma$  confidence of knowing the location of the electrical or magnetic axis with respect to a physical coordinate system figure 3.

The coordinate system is defined using fiducial targets permanently mounted on each sub-assembly. The simplest possible relationship is the shortest vector between the magnetic axis and the coordinate reference frame defined for each assembly. The targeted uncertainty is assumed to include the random and unknown systematic errors of the complete alignment measurements once all systematic errors have been accounted for and corrected. This includes both the magnetic survey and the definition of the assembly magnetic axis, the geometric survey, and the link between the two.

Pre-alignment measurements reported in the literature [5–23] are in general divided into two stages, as shown in figure 4: magnetic measurement or realisation of the magnetic axis, and measurement of magnetic sensor and fiducials location with coordinate metrology (CMMs).

For the magnetic survey, a magnetic measurement system is used to define the location of the magnetic null by best fitting a stretched wire to locate it (see figure 4(a)). In PACMAN, this was achieved by the vibrating wire method [6, 7]. Results from this project showed that the uncertainty of the magnetic survey was in the range of  $3\ \mu\text{m}$  for CLIC magnets [8]. The geometrical survey was achieved using a bridge-type CMM. A contact or non-contact probe was used to measure the relative coordinates of all fiducials mounted on the assembly. This created a dimensional coordinate frame and relationships between the components (see figure 4(b)). To link geometrical and magnetic surveys, the location of the stretched wire was described within the coordinate system as defined by the geometrical survey. In practice, this was achieved by measuring fiducials kinematically linked to the stretched wire. Here, this step was skipped, as the link between the wire and fiducials will be made by measuring both wire and fiducials with the CMM. Two types of measurement heads, namely ‘tactile’ for fiducials and ‘non-contact’ for the wire, were used by the CMM for this integrated procedure [9].

## 2. State of the art

A summary and comparison of stated accelerator alignment measurement uncertainties of different state-of-the-art work [6, 10–27] were reported by the technology (TE) department of CERN [6]. The claimed uncertainty ranges ( $20\ \mu\text{m}$ – $60\ \mu\text{m}$ ) for metre-plus sized assemblies of both geometrical survey and magnetic measurement uncertainties were investigated. In general, the uncertainties reported were found to be used in a broad sense as the best-case scenario achieved. Based on the reviewed literature, a common practice in building the uncertainty budget is to use the Maximum Permissible Error for length measurement (MPEE) from CMM manufacturers as a quantification of the geometrical survey of the metrology equipment. However, this qualification parameter does not include the real uncertainty of their specific measurement or task-specific uncertainty [28, 29]. For projects studied in [6], this was considered to be an adequate statement of their measurements, as their targeted uncertainty budgets were in the range of ( $20\ \mu\text{m}$ – $60\ \mu\text{m}$ ) for metre-sized magnet assemblies. These targets are achievable using the available high-performance CMM systems such as the Leitz PMM-C Infinity ( $\text{MPEE} = 0.3\ \mu\text{m} + L/1000\ \mu\text{m}$ ,  $L$  in mm) [4].

The ‘task-specific uncertainty’, as defined in the field of coordinate measurement, is a complete uncertainty statement that takes into account all the error sources associated with all the details of the measurement process [30]. Such statements can be produced by several methods as accepted by ISO international standard for evaluation of uncertainties in measurement (GUM) [31]: expert judgement, sensitivity analysis, substitution via calibrated objects, or computer simulation [30].

In recent studies on alignment uncertainties from the Brazilian Synchrotron Light Laboratory (LNLS) [32], CMM alignment measurements uncertainties of both contact and non-contact probe heads were performed using a calibrated artefact. The alignment target for the 1.8 m assemblies was quoted as a  $40\ \mu\text{m}$  error and not as uncertainty; no confidence interval was given. A near metre-long invar alloy beam was machined and calibrated. The calibration uncertainty of this artefact was estimated to be  $2\ \mu\text{m}$ – $3\ \mu\text{m}$  at  $20\ ^\circ\text{C}$  by measuring it with a Carl Zeiss Prismo ultra CMM claimed to have integrated ‘Virtual CMM’ software. Following this initial calibration of their artefact, the length measurement errors (calibration versus measured) on the CMMs used for fiducialisation were evaluated, combining non-contact and tactile sensors. It was found that single-length measurement errors between the artefact calibration and different metrology equipment (CMMs, laser trackers and theodolites) were within the MPEEs given by their manufacturers. However, the calculation or prediction of the full ‘task-specific’ uncertainty of each CMM was not shown. Details were missing of the specific CMM and probe head uncertainties for the different tools, thermal effects, targets form error, and others [32]. This might not be adequate when the tolerances studied are at the limit of the metrology performance. The fixed size and shape of the artefact restricted the study to assemblies with the same shape and dimensions. Other limitations are the high cost of

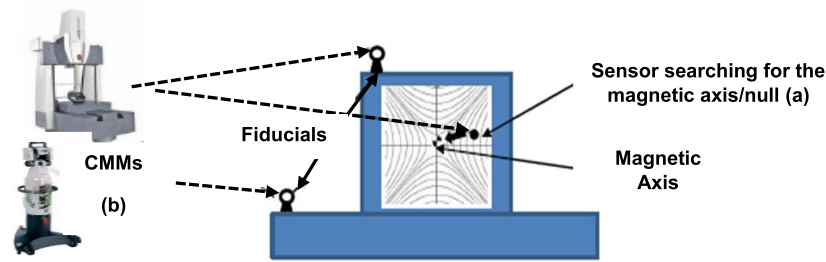


Figure 4. Pre-alignment as a combination of magnetic (a) and geometrical surveys (b).

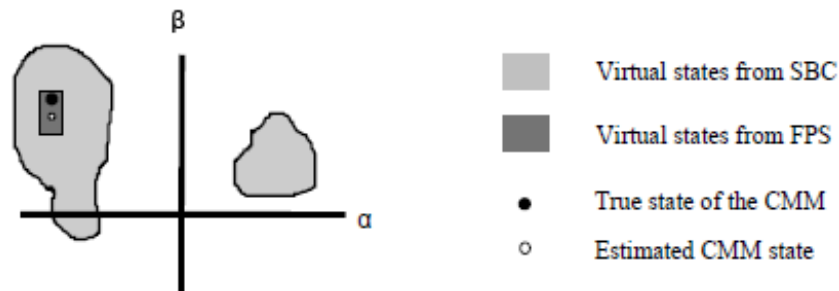


Figure 5. Schematic of 2D state space of possible CMM error map. Reprinted from [35], courtesy of the National Institute of Standards and Technology, US Department of Commerce. Not copyrightable in the United States.

each particular artefact development, manufacture calibration, and the lengthy iterative procedure required for complete task-specific uncertainty evaluation.

In the case of CLIC, a practical industrial scalable method is required. It should be able to quantify *accurately* and should be *traceable* to the international unit of length of the task-specific measurement uncertainty. Such a method must be (1) practical, thus not requiring extensive on-site uncertainty evaluation experiments and expertise, and (2) scalable, for various assembly sizes, geometries, and CMM models and sizes. This would provide a key tool with which to achieve demanding alignment requirements at the required scale. In this work, we demonstrate that the use of a stochastic modelling method as calibrated by standard ISO tests and validated using a common artefact can be a suitable solution.

### 3. Alignment measurements uncertainties prediction by simulation by constraints method

The GUM Supplement 1 standard [33] provides one of the best methods with which the uncertainty of complex metrology measurements can be obtained (i.e. CMM alignment). Using this standard, the measurement can be represented by a mathematical model. Several commercial and research software packages follow the standard. The two most notable pioneering works on which the state of the art is based are the 'Virtual CMM' (initially developed at PTB Germany) [34] and 'simulation by constraints' (SBC; initially developed at NIST USA) [35]. The main difference in the two approaches is the way in which the various error contributors (geometrical CMM errors, form errors, and extrinsic factors) are evaluated and mapped.

For example, the Virtual CMM method relies on full and detailed parametric study of the various errors. This is the so-called estimation of full parametric space (FPS). This can be

performed using several techniques (by substitution of known geometry of calibrated artefacts, laser interferometry and triangulation, or even statistical history error database creation [36, 37]). This, however, involves complex procedures demanding expert knowledge and specialised equipment available at national institutes and metrology R&D centres, rather than commercial metrology laboratories.

The SBC method takes a different calibration approach. It uses information on machine performance that is already available, in the form of the standard machine test qualifications such as ISO 10360 series MPEE, MPEml, MPEms, and MPEmf [38] (table 2). This is done as explained further in (figure 7). Although not as accurate in mapping machine error states as an FPS approach (see figure 5), SBC is still reported to predict accurately CMMs task-specific measurement uncertainty [39]. This, combined with its practicality, availability as existing commercial software [40, 62] and ease of implementation (based on the standard tests part of CMM calibration routines), made it a prime candidate for the current study.

In this work, CMM uncertainty modelling is performed as shown schematically in figure 6.

The final measurement result and its associated uncertainty are functions of three general factors. The first is the difference (variance and band bias combined) between the '**Virtual CMM measurement**' probabilistic model in our case calibrated by SBC method and the '**Real CMM measurement**' as one can observe in figure 6. The other two factors are the **test uncertainty of the standard (artefacts)** used to calibrate the virtual CMM model and the **measured targets drift/stability**. The '**Virtual CMM measurement**' probabilistic model used was mainly a function of the **CMM hardware errors** (which include the 21 geometrical error parameters for a Cartesian-type CMM [17] and the repeatability of the sampling probe head) and **measured targets shape errors**. They consist of 18 rigid body errors (6 degrees of freedom

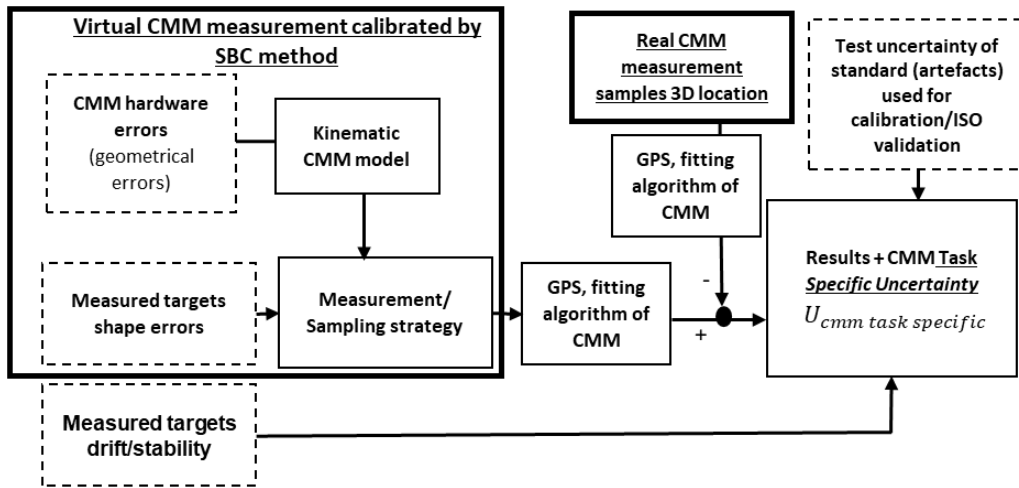


Figure 6. Factors and measurement model affecting task-specific uncertainty of CMM measurements [29].

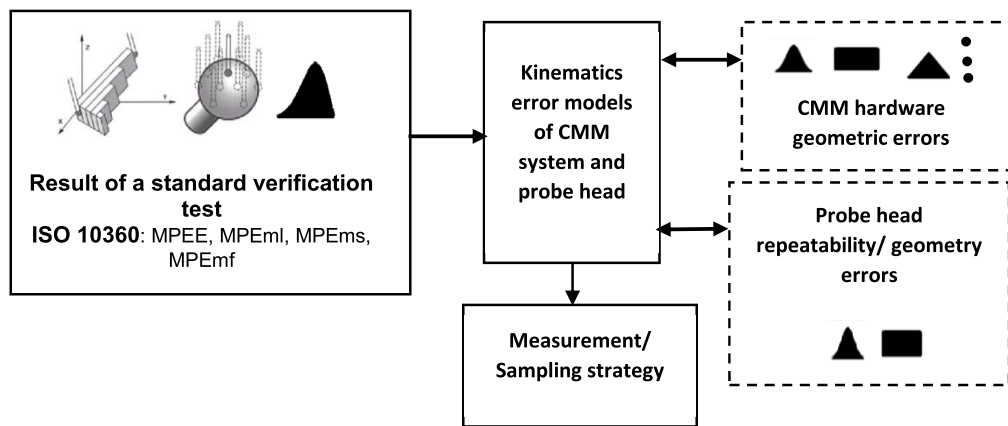


Figure 7. Use of standard tests results in order to map CMM and probe head parameters PDFs using their kinematic models—SBC method [29, 35, 42].

error functions  $\times 3$  axes of the Cartesian machine) and three errors of perpendicularity between each axis. These errors are for a fixed non-articulating touch probe, and their effect on the touch probe location in space can be propagated with the use of homogeneous forward kinematic equations [41]. If an articulating touch probe is used, an additional homogeneous matrix kinematic model that adds the additional DoF of the articulated probe to the end tip location error is required. Each machine has a unique set of such errors, which are a function of the quality of its design, manufacturing techniques applied, materials used, and several other operational factors. Their combined effect is defined as the uncertainty contributor due to the CMM hardware.

The virtual CMM model calibration required an evaluation of the contribution of (A) **CMM hardware errors** and (B) **measured targets shape errors**. Those were defined as probability density functions (PDFs). The **CMM hardware errors** were calibrated by the SBC method, as graphically shown in figure 7 and further explained. The various error source PDFs were propagated through the virtual CMM model to define a resulting PDF quantifying the variance in location of each sample coordinate of the measurement plan as a function of the input parameters' variance [29].

The 21 geometric error parameters (**CMM hardware errors**) for the particular machine were mapped using the SBC method (figure 7).

The methodology behind the SBC is to have a good initial guess of the output performance of the system; namely, the length or location measurement. Such an initial guess can be obtained by already available results of a CMM standard qualifications test, such as that defined in the ISO 10360 series. They can provide quotations for the CMM volumetric performance (MPE) and the touch probe characteristics (MPEml, MPEms, MPEmf) (table 2). They are used to backwards map the CMM input parameters (the 21 CMM geometrical error parameters and probe head repeatability). This is done via an iterative one-to-many optimisation state space search for the defining input parameters PDFs having the output parameters (standard tests results), using the CMM kinematics error model as propagation function. This can be done by following the methods of inverse kinematics analysis [41] commonly used in domains such as robotics. The homogeneous matrices describing the input–output relationship in CMM kinematics can be used algebraically, to solve and find the input parameter values that can give the measured output. This solution is done iteratively, following the Monte Carlo sampling method,

as the output (MPE, MPEml, MPEms, and MPEmf) is not given by a single value but by PDFs which are accepted to be produced by the CMM input parameters' PDFs. At each iteration, a new and unique value combination of the input error parameters is randomly chosen. As the solution of the kinematic equation can be a function of highly improbable or impossible combinations of input parameters (negative planarity errors combined with larger positive), the process is regulated by a set of feasibility constraints; hence the name of the method. The feasibility constraints of the input parameters (21 CMM geometrical error parameters and probe head repeatability) are set as tolerance bands around each separate parameter, where only those algebraic solutions lying within those bands are accepted, and all others are rejected as not physically feasible outliers. The known output (MPE, MPEml, MPEms, and MPEmf), also referred to in the literature as bounding measurement sets (BMS) [35, 42], can be used to set the limits of the input parameters. For example, if the volumetric performance of the CMM is better than 10  $\mu\text{m}$ , then this is a good guess for the maximum straightness error band, which is highly unlikely to be much larger than 10  $\mu\text{m}$ . The more measurements and information there is in the BMS, the more stringent can be the parameter constraints, and the more the SBC results converge from the higher side to the FPS, but always slightly overestimating them. This inherent slight overestimation to the FPS can ensure that the real uncertainty would be always captured within the SBC uncertainty predictions.

Following this strategy, the CMM model's possible error sources (for CMM hardware geometric errors and probe head repeatability) are finally mapped in the form of PDFs. Once those are determined, the kinematic model of the CMM and the touch probe can be used to propagate forward, via Monte Carlo sampling, the coordinate uncertainty for each probe sample to any measured position within the CMM volume directed by any measurement plan (see figure 7).

**Measurement targets shape errors** represent the error influences due to the imperfections in the geometry of the reference targets that are measured. The uncertainty of the real shape of the reference targets can create an unknown bias in CMM measurement samples and can be propagated through the measurement model [43–45].

For example, a common practice in the high-precision alignment of magnets is to use the reference targets, which are reference spheres permanently integrated into or mounted on the assembly. The uncertainty value of their shape can be estimated as the maximum form error given by the manufacturer. This can be defined as side  $a_s$  of a square-shaped uncertainty ( $U_{sh} = \frac{a_s}{\sqrt{3}}$ ) quantifying the uncertainty due to the shape errors.

**Test uncertainty of standard** is the combined uncertainty of knowing the dimensions of the traceable artefacts used to perform the ISO 10360 standard test and CMM calibrations as specified in [46, 47]. This includes uncertainties due to the sole calibration of the artefacts used,  $U(\text{art.calib.})$ ; the unawareness of the exact thermal expansion coefficient of the

artefact used,  $U(\text{art.}\alpha)$ ; the uncertainty of the artefact temperature during the test performance,  $U(\text{art.}T)$ ; and uncertainties caused by the fixing and orientation of the artefact,  $U(\text{art.Fix})$ :

$$U_w = \sqrt{U^2(\text{art.calib.}) + U^2(\text{art.}\alpha) + U^2(\text{art.}T) + U^2(\text{art.Fix})}. \quad (1)$$

The final class of uncertainty contributor is the **measured targets drift/stability**. This category includes all other influencing factors that could include an unknown bias within the measurement procedure. One of the most influential factors in metrology and precision engineering is the thermal effect [48–52]. This could create an unknown dimensional bias in both the CMM and the measurand which peaks when biases are in opposite phases [48, 53]. As modern high-end CMMs have integrated thermal error compensation and thermally stable reference scales, the stability of the measurand can be accepted as a main influencing factor [28, 52, 53]. This can be evaluated experimentally by repeated measurements of the assembly at different times and energy (thermal) states: once at a thermally 'soaked' room condition steady state and once with magnets and any other active system (possibly concentrated heat sources) switched on at the end of full-day measurement [53].

Measurement coordinates depend on the coordinate frame assumed, which in itself can be unstable due to drift. Thus, a direct coordinate comparison could give false information. As an alternative, the authors of the current paper suggest a direct comparison of fixed distances (between reference targets on the granite support and the assembly fiducials). The 3D distance between rigid bodies is independent of the coordinate frame assumed, and any drift in this 3D distance would be due to the measurand drift (or the CMM, if not compensated thermally) in space equations (2)–(4):

$$U_{ex} = \frac{a_t}{\sqrt{3}} \quad (2)$$

$$a_t = \max_{n=r-i} D_{\text{thermal sources off-steady state}} - D_{\text{thermal sources on-steady state}} \quad (3)$$

$$D = \sqrt{\Delta X_{r \rightarrow i}^2 + \Delta Y_{r \rightarrow i}^2 + \Delta Z_{r \rightarrow i}^2}. \quad (4)$$

Here  $\Delta X_{r \rightarrow i}$ ,  $\Delta Y_{r \rightarrow i}$  and  $\Delta Z_{r \rightarrow i}$  are the drifts of each fiducial part of the assembly in  $X$ ,  $Y$ , and  $Z$ ;  $a_t$  is the maximum total drift in 3D among all the fiducials installed between a stable 'soaked' thermal state and a thermal state with possible heat sources switched on, and  $U_{ex}$  is the uncertainty due to fiducial drift taken as a conservative square shape PDF.

The contributing factors of **the CMM hardware errors** and **the measured targets' shape uncertainties** influence the error of each sample measurement, and thus are propagated through the CMM measurement and sampling strategy. The number and distribution of samples are defined along the surface of the measurand (i.e. reference sphere or stretched wire). More samples give a lower uncertainty as the shape of the measurand is better known [43, 45], and thus a smaller bias for its centre location could exist.

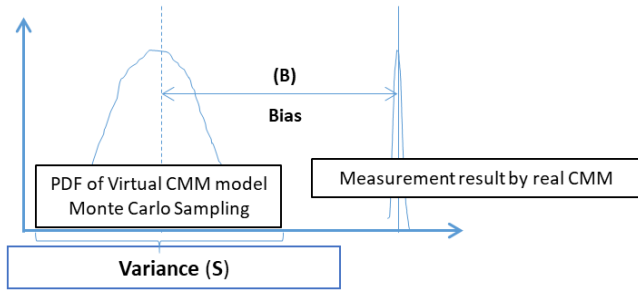


Figure 8. Variance and bias of virtual CMM model.

Once the magnitude of the error sources has been determined, the CMM virtual model is used to sample interactively, by Monte Carlo method, from the PDFs of the **CMM hardware**, and **measured targets shape errors**. In this way, they are propagated through the CMM software fitting algorithm according to the task set by the metrologist in the language of geometric product specification (GPS) [54]. The output is a PDF with variance ( $S$ ) describing the possible location of the measurand feature (figure 8).

The error between the PDF (describing the possible location of the measurand feature by virtual CMM) mean value and the one measured by the CMM system value defines the bias ( $B$ ) due to its **CMM hardware** and **measured targets shape errors** (figure 8).

The Virtual CMM model variance  $S$  and bias  $B$  (figure 8) test uncertainty  $U_{tu}$  can give a quantification of the CMM-specific uncertainty equation (5) [55], where  $k$  is the expansion coefficient for the significance level  $\sigma$  (i.e.  $1\sigma$ ,  $2\sigma$  or  $3\sigma$ ):

$$U_{\text{cmm specific}} = S * k + B + U_{tu}. \quad (5)$$

The measurement task might require the use of a multisensory CMM. This would imply the use of sensorial heads based on different working principles, i.e. tactile, non-contact linked in the same dimensional reference frame. On such occasions the  $U_{\text{cmm specific}}$  has to be extended to include any calibration offset between the different types of sensors used  $O$  [56–58] (see equation (6)):

$$U_{\text{cmm specific}} = S * k + B + O + U_{tu}. \quad (6)$$

Such an offset ( $O$ ) can be evaluated as the  $L_{\text{Dia},n \times 25::\text{MPS}}$  in ISO 10360-9 (maximum permissible multiple probing system location error for  $5 \times 25$  point sphere fit) [59] under certain assumptions. The  $L_{\text{Dia},n \times 25::\text{MPS}}$  result of an ISO 10360-9 test is a function not only of the offset ( $O$ ) between two probes (based on different working principles) but includes errors due to the CMM geometry. Thus, the use of  $L_{\text{Dia},n \times 25::\text{MPS}}$  as the probes offset ( $O$ ) would provide a small overestimation. Such an assumption, however, can be accepted as correct, as suggested by the ISO procedure for uncertainty management (PUMA) method [60], as long as  $U_{\text{cmm specific}} < U_{\text{targeted}}$ . If this is not the case and  $L_{\text{Dia},n \times 25::\text{MPS}}$  contributes a significant amount to  $U_{\text{cmm specific}}$ , a more thorough investigation for the exact value of  $O$  should be performed.

The task-specific uncertainty of assembly measurements (performed at the metrology laboratory) can be quoted as the uncorrelated sum of the specific uncertainty of the CMM

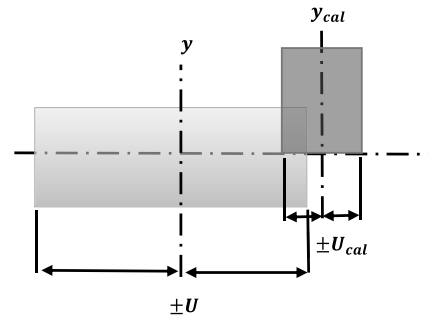


Figure 9. Combining uncertainty regions of artefact and model used for validation.

system ( $U_{\text{cmm specific}}$ ) combined with the uncertainty linked to the assembly stability  $U_{ex}$  during measurement:

$$U_{\text{task specific}} = \sqrt{U_{\text{cmm specific}}^2 + U_{ex}^2}. \quad (7)$$

The final stage is to validate the uncertainty prediction. A calibrated stable artefact, with targets (fiducials) of similar shape and size to that used on the assembly, and distributed at similar distances, is measured accurately. The maximum 3D location errors calculated between the calibration certificate of the artefact and the measurements performed by the studied CMM are compared. A final judgment of the accuracy of the task-specific uncertainty prediction by the software can be calculated using equation (8) defined in ISO/TS 15530-4 [58] as a comparison of the overfall ratio between the uncertainty of the reference standard and the predicted by a model uncertainty (figure 9):

$$\frac{|y - y_{\text{cal}}|}{\sqrt{U_{\text{cal}}^2 + U^2}} \leq 1. \quad (8)$$

In equation (8),  $y$  is the measurement result,  $y_{\text{cal}}$  is the artefact calibrated value,  $U_{\text{cal}}$  is the expanded uncertainty of the calibrated artefact, and  $U$  is the modelled expanded task-specific uncertainty.

#### 4. Results

In our study, the measurement task of alignment was defined as achieving the required location tolerance of either a sphere or a thin ( $100 \mu\text{m}$ ) cylinder representing the magnetic measurement reference wire (figure 10).

The shortest magnet assembly is the T1 module, with a length of 0.54 m between the furthest alignment fiducials. The longest magnet assembly is a T4 module, which has a length of 2.1 m between the furthest fiducials. The magnet assembly has a minimum of four alignment fiducials, of which three are required for a dimensional frame reference (DFR) definition. The DFR is created as a system of specified datums (A/B/C) as defined in [61]. The alignment tolerances are represented as a GPS location tolerance zone around the most distant sphere or cylinder (computer aided design (CAD) representing the fiducials or stretched wire) from the DFR defined by another three sphere fiducials installed on the assembly (figure 10).

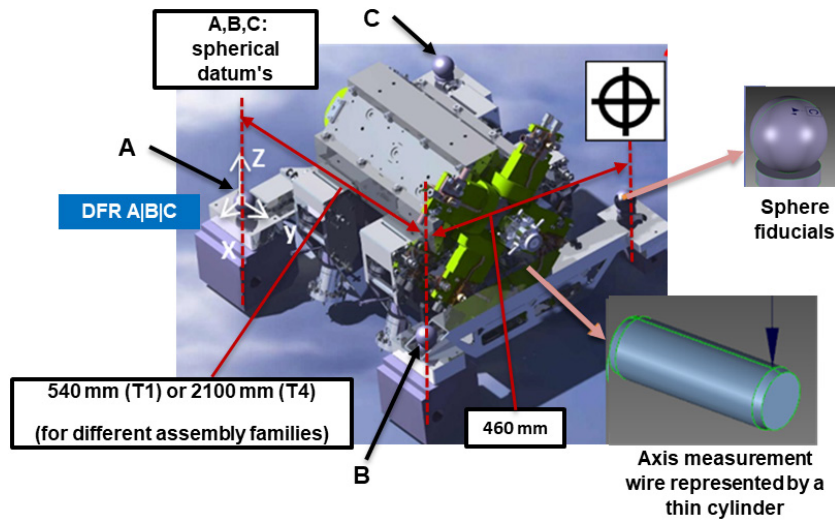


**Figure 10.** Magnet assembly and GPS language task example with four alignment fiducials.

**Table 1.** Evaluated shape errors of measurement targets for determination of  $U_{sh}$  contributor to the task-specific uncertainty.

|  | Best measured ( $\mu\text{m}$ ) | Worst measured ( $\mu\text{m}$ ) | Sphericity ( $\mu\text{m}$ ) |
|--|---------------------------------|----------------------------------|------------------------------|
| Fiducials used (PACMAN experiment)             | $x$                             | $x$                              | 1                            |
| 100 $\mu\text{m}$ diameter CuBe stretched wire | 1.76                            | 2.93                             | $x$                          |

**Table 2.** CMM and probe heads used for uncertainty study based on ISO 10360-5 and ISO 10360-9 qualification and specification (Room environment: Class 1;  $\pm 0.1$  °C).

|                | MPEE<br>( $\mu\text{m}$ ) | MPEml<br>( $\mu\text{m}$ ) | MPEms<br>( $\mu\text{m}$ ) | MPEmf<br>( $\mu\text{m}$ ) | Non-contact wire probe<br>head repeatability on<br>cylinder location<br>( $\mu\text{m}$ ) | Non-contact<br>wire probe head<br>MPS/MPE<br>( $\mu\text{m}$ ) | Largest distance<br>sphere to sphere<br>(m) | Stylus<br>length<br>(m) |
|----------------|---------------------------|----------------------------|----------------------------|----------------------------|---|--|---|-------------------------|
| Leitz Infinity | $0.3 + L/1000$            | 0.62                       | 0.13                       | 1.02                       | 0.7   | 3  | 0.63  | 0.080                   |
| Zeiss PRISMO   | $1.9 + L/400$             | 1.70                       | 1.10                       | 2.30                       | 0.7   | 3  | 2.10  | 0.080                   |

L is in mm.

MPEE = Maximum permissible error for length measurement.

MPEml = Largest range of centre coordinates for the  $5 \times 25$  point spheres fit.

MPEms = Deviation of the 125-point sphere fit diameter from calibrated diameter.

MPEmf = Range of residuals of the 125-point sphere fit.

MPS/MPE = Maximum permissible multiple probing system location errors for the  $5 \times 25$  point sphere fit.

First, we studied the uncertainty of defining the location of the furthest fiducial in the assembly DFR. Then, we carried out the final alignment measurement uncertainty of the magnetic axis, which included magnetic measurement, non-contact measurement of the wire, and tactile measurement of the sphere fiducials. A commercially available software package, PUNDITCMM™, which implements the SBC method, was calibrated from measurements and used [22, 26]. The evaluated shape errors of the targets measured (spheres and stretched wire) are summarised in table 1.

The standard test data used for the calibration of the CMM hardware geometric errors model are shown in table 2.

The data concerning the Leitz Infinity CMM [4] was taken from the standard verification tests performed by the manufacturer on site during the annual checks. The ISO tests were performed with Zerodur artefact with  $\text{CTE} = 0.1 \mu\text{m m}^{-1}$ . Thus, for the Class 1 room environment,  $U_{tu}$  was estimated to be less than  $0.02 \mu\text{m}$ .

The data for the Zeiss PRISMO CMM was taken from the manufacturer's quoted performance of their Zeiss PRISMO ULTRA 16/30/10 (capable of accepting objects up to 3 m long within its measurement volume) [63]. It is expected that on-site measurements after calibration can provide better results than those quoted by the manufacturer. Such is the case here, as the number quoted by the manufacturer usually refers to a worst-case scenario based on their experiments with multiple CMM systems.

The performance of a particular CMM can be better (due to a better-controlled environment or lower specific geometrical errors). Thus, the quoted data for the Zeiss PRISMO can be accepted as conservative. The uncertainty of the non-contact measurement probe head was estimated internally at CERN's metrology lab. Its repeatability measurement was performed by measuring the wire surface in two small areas and fitting a circle on these results. It was used as a repeatability measurement of the non-contact sensor, equivalent to the



**Figure 11.** Carbon fibre tetrahedron artefact studied [64, 65]. Reproduced with permission from [65].

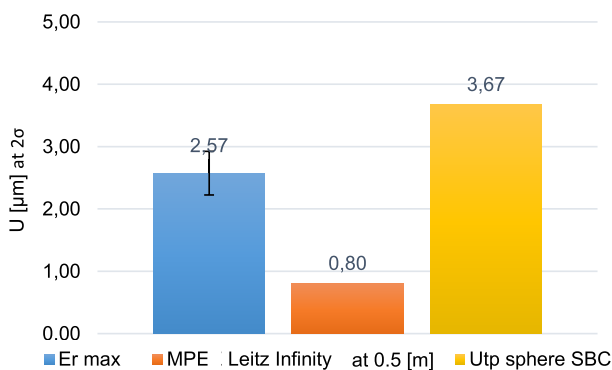


**Figure 12.** Comparison of measured errors versus predicted errors by model uncertainty and MPE of Leitz Infinity CMM for 0.5 m.

MPEml results of the tactile sensors. The MPS/MPE is the maximum offset error between the measurement of the centre of a sphere with the non-contact and tactile sensors defined as  $L_{\text{Dia},n \times 25::\text{MPS}}$  in ISO 10360-9 [59].

#### 4.1. Validation of simulation by constraints uncertainty model

The uncertainty prediction model was validated against a calibrated artefact, as part of an international metrology inter-laboratory study [64]. This artefact has arms of 0.5 m in length, made of carbon fibre-reinforced polymer (CFRP) with a coefficient of thermal expansion (CTE) of  $1 \mu\text{m m}^{-1} \text{K}^{-1}$ . Fiducial spheres are made to a shape tolerance equivalent to grade 5 ISO-3290 sphericity precision, with a maximum roundness error of  $0.127 \mu\text{m}$ . The artefact calibration uncertainty of the distances at  $2\sigma$  was quoted as  $0.7 \mu\text{m}$ . A complete artefact survey was performed and repeated three times using a Leitz Infinity CMM, within the CERN metrology laboratory (figure 11).

The maximum measured location error (*Er max*), the CMM MPEE (provided by Leitz for measured distances of 0.5 m), and the predicted task-specific uncertainty (Utp sphere SBC), are shown in figure 12.

The results (figure 12) show that the measurement errors were within the prediction of the calibrated SBC uncertainty model of the CMM. The *Er max* value includes the artefact calibration uncertainty as an error band. The calculated uncertainty prediction performance (according to ISO test, as shown by equation (8)) is less than 1, being equal to 0.18

(dimensionless), thus passing the validation test for this particular CMM and measurement task. These results confirm, for our applied case, a successful validation of the method as seen in [39, 66]. In previously published state-of-the-art work, the CMM uncertainty modelling (via SBC method) overestimated real measured errors by between 1.3 and 5 times. The ratio depended on the type and shape of feature or fiducial measured and the type of GPS task selected. This overestimation is due to the nature of the method, that uses ambiguous information from the standard test that can be due to a larger state space of errors than the real one associated with a particular CMM. In the current case, a tight ratio was observed between the predicted uncertainty and the measured error. This behaviour can be explained by the physical similarity of the tetrahedron spheres, the magnet fiducials (high precision spheres) with the standard tests used for ISO qualification, and the calibration of the model (high-precision spheres). We used this model, as validated, to study the expected task-specific measurement uncertainty of both the smallest and largest assemblies of CLIC (T1 and T4 respectively).

#### 4.2. Alignment measurements uncertainty prediction of 0.6 m T1 assembly

The alignment set-up of the PACMAN T1 magnet assembly prototype is shown in figure 13.

The names and locations of the various fiducials referenced in the study ( $S1$  to  $S21$ ) are shown in figure 13. As shown, the  $S1$  to  $S4$  spheres are mounted on granite;  $S9$  to  $S11$  are mounted on the alignment arm (used to link each assembly to the tunnel alignment reference of a stretched wire [2]); and  $S20$  and  $S21$  are mounted on the top of the steel magnet. As a first step, we evaluated the stability and thermal errors of the measurand. Thermal sensors (including air front measurement sensors and assembly surface temperature) were mounted next to the installed fiducials. Temperatures were recorded during three measurement days, as shown in figure 14.

The full set of CMM alignment measurements on the assembly took a complete workday. After the initial measurement, the weekend gave time for the system to stabilise. During the second measurement day, the magnet was switched on (figure 14, green line). The magnetic measurement engineer of the team [67] defined a minimum current of four amperes as being required for the magnetic axis measurement. No water-cooling was provided to the magnet as it is required only at high amperage operational rates ( $\sim 120$  amperes), due to the Joule heating effect in the resistive coils. The second reason for not providing passive water-cooling was that it could create a thermal gradient (between the coolant in the coils and the ambient air temperature) and act as a concentrated heat source within the assembly.

As expected, switching on the magnet to a minimum current created an internal concentrated heat source. This caused the magnet temperature to start rising during Monday (figure 14, orange). The aluminium arms were influenced by this source as well. However, their temperature followed more closely the peak-to-peak air conditioning bias due to aluminium's lower thermal inertia. The delta drift of the absolute 3D distances

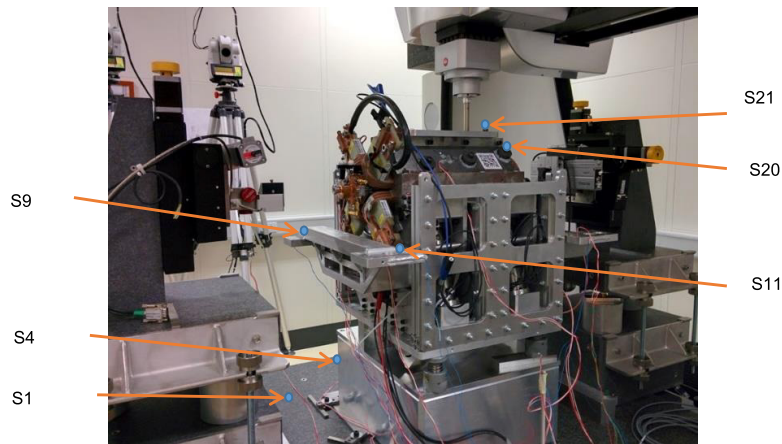


Figure 13. CLIC T1 magnet assembly integrated within CMM.

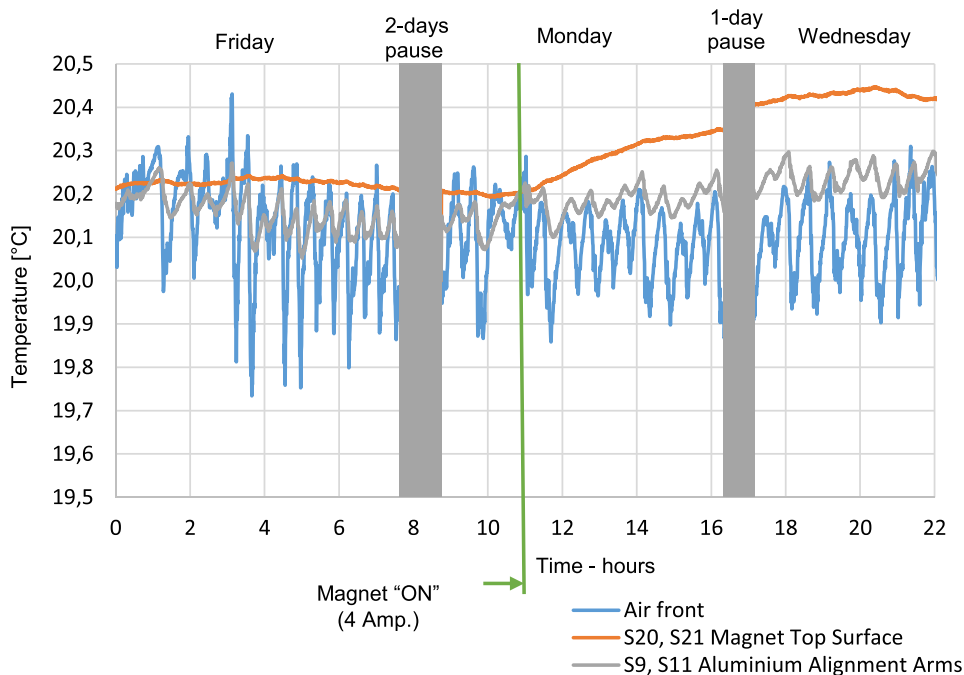


Figure 14. Thermal variation of air, magnet, and alignment arm part of the assembly for the three days of measurements performed. Green represents the time at which the magnet was switched on (4 amperes).

between a reference sphere mounted on the granite CMM base and various spheres mounted on the assembly for two consecutive days of measurement were calculated (figure 15). All measured drifts are normalised to the SI unit for length, the metre.

The initial CMM measurements were performed with no power input into the system as a reference day (Friday). No magnetic axis alignment was performed. The peak drift was recorded between Friday and Monday. The results from Friday to Wednesday showed a reduction of the relative 3D distance drift. We believe this is due to the room air conditioning system active compensation coming into effect. The magnet targets closest to the heat source (magnet coils) have the highest recorded drift (measurements normalised to the metre). The delta normalised drift between the granite base, aluminium arms and the granite magnet has a maximum value of  $2.55 \mu\text{m m}^{-1}$ . This value was used for the estimation of the thermal drift (environment) uncertainty, accepted as the side of a uniform uncertainty

distribution  $a_t = 2.55 \mu\text{m} \times 0.63 \text{ m} = 1.6 \mu\text{m}$  (figure 15),  $U_{\text{ex}} = \frac{a_t}{\sqrt{3}} = 0.92 \mu\text{m}$ . This was added as an uncorrelated uncertainty to the task-specific uncertainty budget further shown in figure 17. The calculated MPEE of the Leitz Infinity machine, for the furthest measured distance on the T1 assembly ( $0.95 \mu\text{m}$ ), is significantly less compared to the modelled tactile measurement uncertainties of a fiducial sphere location with respect to a three-sphere dimensional reference frame ( $3.81 \mu\text{m}, 2\sigma$ ), as shown in table 3.

This study was performed for the calibration data of the Leitz Infinity CMM (table 2), measuring available and mounted spheres on a T1 assembly with a shape tolerance of  $1 \mu\text{m}$  (table 1). The modelled tactile uncertainty for a sphere location was found to be significantly larger than the MPEE given by the manufacturer ( $3.81 \mu\text{m}, 2\sigma$  versus  $0.95 \mu\text{m}$ ). This study accounts only for the CMM geometric machine errors, contact probe heads repeatability and feature form errors. It is important to note that this study does not include the magnetic

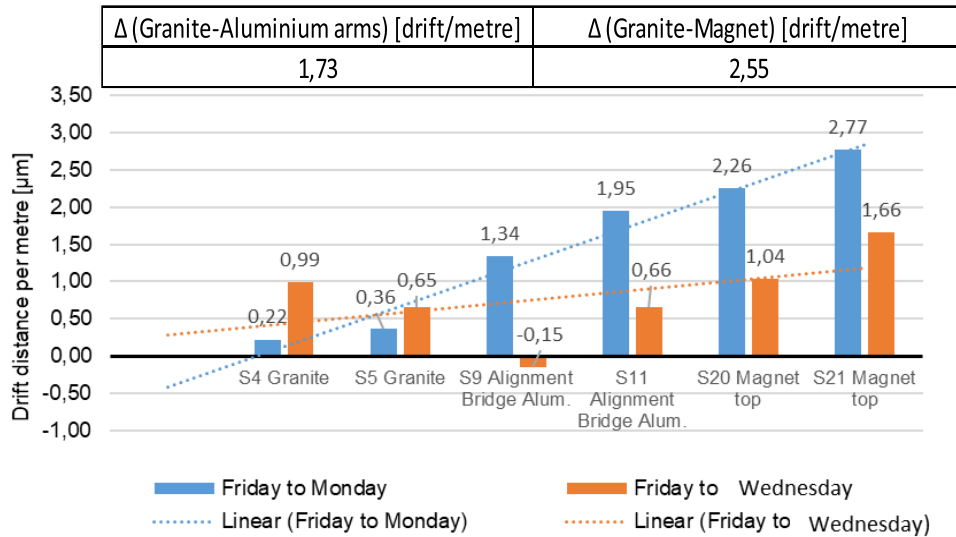


Figure 15. Spheres (normalised to the unit length of metre) 3D drift for various locations on the assembly for two consecutive days.

Table 3. MPEE of Leitz Infinity for the furthest distance on the assembly versus alignment measurements uncertainty of sphere in three-sphere reference datum.

|          | MPEE at max distance of 0.63 m | $U(2\sigma)$ sphere location in three-sphere datum |
|----------|--------------------------------|--|
| $U$ (µm) | 0.95                           | 3.81   |

measurement, nor thermal errors, nor non-contact sensor repeatability and offset error contributors. The results of the model are represented in a  $2\sigma$  (95%) coverage interval, as suggested as standard in [68].

The effect of fiducial grade (shape form error) on the tactile measurement uncertainties was studied in more detail. The same model from the previous study was run for fiducials with varying form errors and specification. The results are highlighted in figure 16.

It was observed that uncertainty significantly increases as a function of the shape quality of fiducial spheres. For example, using the highest commercially available grade spheres (ISO-3290), with a  $0.13 \mu\text{m}$  form error, can lower the alignment measurement uncertainty by  $0.5 \mu\text{m}$  to a total of  $3.36 \mu\text{m}$ . However, using spheres of poorer quality ( $5 \mu\text{m}$ ), sphericity can rise by  $3.36 \mu\text{m}$  to a total of  $7.23 \mu\text{m}$  (figure 16).

As a final study, the task-specific alignment uncertainty of defining the location of the magnetic axis in the three-sphere assembly datum (figure 17) was studied (blue,  $6.91 \mu\text{m}$ ). This was compared to the MPEE (black pattern) and all other major uncertainty contributors.

The task-specific uncertainty itself is the sum of all correlated and uncorrelated sources. The uncorrelated error sources are the magnetic measurement, thermal drift wire measurement, and datum measurement. The offset between tactile and non-contact sensors can be conservatively accepted as a bias value equal to the worst value of the MPS/MPE tests ( $3 \mu\text{m}$  table 2, orange in figure 17). Thus, it is accepted as completely correlated and directly added to the quadratic sum of the rest. Such a conservative approach of bias addition (for the probes offsets) can be accepted, and as suggested by the PUMA

method [60], such practice is acceptable as long as the final task uncertainty is lower than the targeted one. Wire standard measurement uncertainty was modelled ( $1.34 \mu\text{m}$  ( $1\sigma$ ); grey in figure 17) using a measurement model calibrated (by the SBC method) for the non-contact sensor mounted on a tested Leitz CMM with measured repeatability of finding the centre of cylinder =  $0.7 \mu\text{m}$  (see table 2). The datum uncertainty was defined and later estimated as the location tactile measurement uncertainty of a sphere, part of a three-sphere defined datum for the same CMM and tactile probe equal to  $3.81 \mu\text{m}$  ( $2\sigma$ ) (see table 3). The thermal uncertainty was also estimated experimentally for the assembly (figure 15). The magnetic measurement uncertainty is as found by our magnetic measurement expert studies and quoted in [8]. The results are given at  $1\sigma$  in relation to the  $12 \mu\text{m}$  targeted standard alignment uncertainty defined as well at  $1\sigma$ .

This study shows that the MPEE given by the manufacturer is not a correct reference for the quotation of alignment measurement uncertainty. The MPEE underestimated the assembly expanded ( $2\sigma$ ) measurement uncertainty ( $13.81 \mu\text{m}$ ) by a factor of nearly 15 for CLIC T1 module CMM measurements.

#### 4.3. Alignment measurements uncertainty prediction of 2 m T4 assembly

A CMM measurement model (based on the SBC method) was calibrated using the ISO 10360-5 data of a Zeiss PRISMO CMM (capable of holding an assembly up to 3 m) (table 2). The MPEE of this machine for the furthest distance on the assembly, and the modelled tactile measurement location uncertainty of a sphere defined in another three-sphere dimensional reference frame, are compared as shown in table 4.

The standard uncertainty of a sphere location ( $4.10 \mu\text{m}$ ,  $2\sigma$ ) is lower than the MPEE given by the manufacturer  $4.10 \mu\text{m}$ . As expected, the results for the location uncertainty are higher than the T1 results, but not by a large amount. The MPEE, in this case, covers the predicted sphere alignment uncertainty. Thus, it can be concluded that the alignment measurement uncertainty is not directly proportional to the assembly size

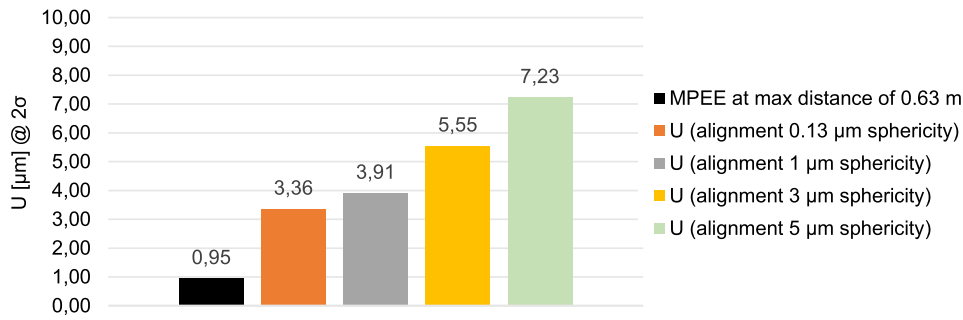


Figure 16. Variation of alignment uncertainty as a function of fiducials form errors.

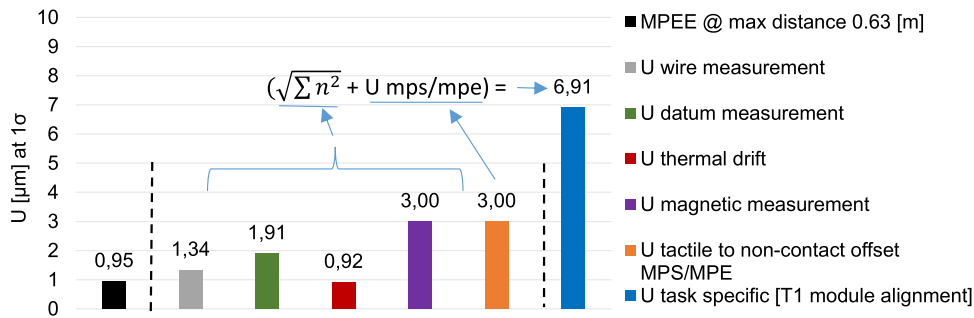


Figure 17. Final alignment uncertainty of magnetic axis alignment measurements using the three spheres datum of CLIC T1 assembly and respective quadratic contributors.

Table 4. MPEE of Zeiss PRISMO CMM for the furthest distance on the assembly versus prediction by model alignment measurements uncertainty of sphere in three-sphere datum.

|        | MPEE at max distance of 2.1 m | U(2σ) sphere location in three-sphere datum |
|--------|-------------------------------|---|
| U (μm) | 4.70                          | 4.10  |

as the MPEE. On occasions, the MPEE can cover the tactile location measurement uncertainty, and on other occasions it cannot. This model does not include all additional uncertainty contributors, such as the thermal drift errors.

The predicted complete task-specific uncertainty is shown in figure 18.

The final task-specific uncertainty for the location of a magnetic axis within the magnet assembly coordinate frame is 7.96 μm at 1σ. It corresponds to the sum of all correlated and uncorrelated sources. The uncorrelated error sources are the magnetic measurement, thermal drift wire measurement, and datum measurement. Those are summed in the same way as the study for T1, as shown in figure 17. The T4 assembly module prototype is not yet produced and the non-contact sensor used has never before been integrated with the Zeiss machine. We, therefore, took into account the following assumptions for this analysis. Firstly, the tactile to non-contact offset is assumed to be the same as that measured at the Leitz Infinity. Secondly, the thermal effects for the T4 assembly would be linear, increasing from T1 due to the longer size of the assembly. Both assumptions can be confirmed once the T4 assembly is available for experimentation. The main variation of the T4 results with respect to the T1 is related to the expected increased thermal drift (3.1 μm extrapolated from the 2.55 μm m<sup>-1</sup> experimental results for T1). Tactile location measurement uncertainty has minimal variation, from

1.91 μm (figure 17) for T1 to 2.05 μm for T4 (figure 18). In this study, the MPEE fails again to cover the expanded (2σ) task-specific alignment uncertainty (15.92 μm), by a factor of three.

#### 4.4. Uncertainty budget for accelerator assembly at underground tunnel

If alignment measurements have to be carried out within an accelerator tunnel under real thermal operational conditions of the machine (i.e. full magnet power of ~120 amperes +, water-cooling, and air ventilation), accurate corrections to the systematic offsets will have to be applied. Systematic offsets are expected, in the order of hundreds of microns, due to large thermal gradients between alignment measurements and operational conditions (i.e. gradients of +20 °C). The remaining uncertainty budget, for thermal errors compensation, was calculated as the uncorrelated remaining quadratic contributor to the target of 12 μm, as shown in table 5.

The uncertainty budgets left over for any additional error sources from the targeted alignment uncertainty for the T1 and T4 assemblies are 8.89 μm and 9.80 μm respectively, at 1σ. These can be accepted as the targeted uncertainty for any future tunnel thermal drift effects compensation.

#### 4.5. Conclusions

The SBC method following the GUM Supplement 1 standard was successfully validated for accurate uncertainty prediction of spherical fiducials location, using an independently calibrated artefact from an inter-laboratory study. This model was used to predict sphere fiducials alignment measurement uncertainties for both T1 and T4 CLIC modules. Thermal

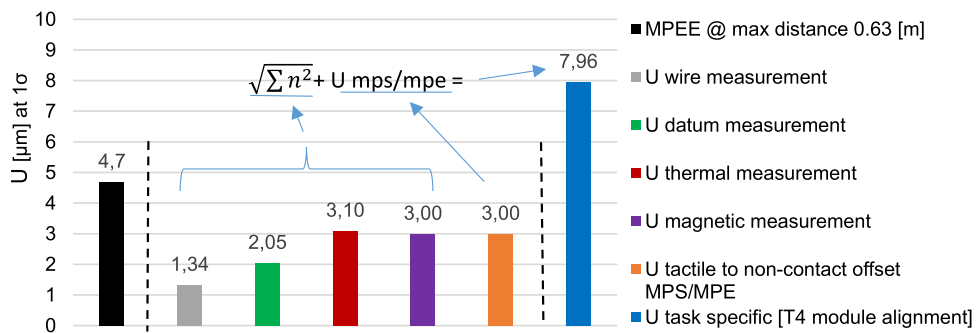


**Figure 18.** Final alignment uncertainty of magnetic axis of CLIC T4 assembly and respective quadratic contributors.

**Table 5.** Uncertainty tolerance left over for any additional uncorrelated error sources from targeted alignment uncertainty.

|                                    | $U$ budget left for T4 | $U$ budget left for T1 |
|------------------------------------|------------------------|------------------------|
| $U$ at $1\sigma$ ( $\mu\text{m}$ ) | 8.98                   | 9.80                   |

drift, due to a concentrated heat source (magnet coils) within the assembly during CMM measurement, was successfully quantified for a T1 type CLIC assembly. It was extrapolated to predict the effect for the larger T4 assembly as no complete prototype currently exists.

The two most sensitive factors influencing the task-specific uncertainty for such alignment procedures are the form error of the measured targets and the geometrical thermo-mechanical stability of the assembly. For both 0.54 m and 2.1 m assemblies, the complete task-specific uncertainty is within the alignment tolerance of CLIC of  $12 \mu\text{m}$  at  $1\sigma$ . However, these are valid only for the laboratory conditions under which the measurements were performed. An uncertainty tolerance of  $8.98 \mu\text{m}$  for T4 and  $9.8 \mu\text{m}$  for T1 is left over for any thermal drift compensation applied for alignment of the machine at nominal tunnel operation conditions.

The presented results show that the usual practice of using the standard specification of the metrology equipment, such as the maximum permissible length error (MPEE), as the expected uncertainty for the alignment measurements of magnet assemblies, is not a correct approach. The task-specific uncertainty in the cases of both T1 and T4 is significantly larger than the MPEE. This is due to the mixture of sensors used (non-contact, contact, magnetic measurement) and due to the presence of thermal load within the assembly. Also, MPEE was shown to misrepresent the tactile location measurement uncertainty for the T1 module. Even without additional error sources, it would be inadvisable to trust this value in tight alignment error budgets made for complex assemblies.

When alignment measurements of large assemblies are required at high accuracy, the task-specific uncertainty should not be ignored and substituted with reference test values such as the MPEE. The application of the SBC method for virtual CMM model calibration, combined with reference drift measurements, showed promising results. It is a viable methodology that can deliver accurate task-specific uncertainty measurements at the industrial scale required by CLIC.

One recommendation for future CLIC alignment studies would be to validate the uncertainty prediction of the stretched wire non-contact measurements in a datum created by tactile measurements of fiducials or precision spheres. This can be done by designing a thermally stable artefact, linking a  $100 \mu\text{m}$  diameter cylindrical artefact to reference spheres in dimensions similar to the studied assemblies. The artefact should be calibrated to low uncertainty (below  $1 \mu\text{m}$  at  $2\sigma$ ) by a national institute providing traceability to the metre SI unit realisation [5]. The T4 assembly extrapolation results should be confirmed experimentally once a fully operational T4 prototype is available. Further reproductions of the studies for a different type of fiducials, measurand dimensions and CMM types could be recommended. Further studies and inter-comparison of uncertainty modelling based on the full parametric state (FPS) strategy against simulations by constraints (SBS) (figure 5) for CMM model calibration can be performed. This could provide more accurate results in future, with the further development and commercialization of high-precision error mapping systems, such as one based on micro-triangulation and ultra-precise interferometry [69].

## Acknowledgments

The research leading to these results has been coordinated by CERN and Cranfield University under the PACMAN project [70] framework. We would like to thank the people of the European Union providing the financial support for the PACMAN project and for this current work in the form of grant agreement ITN-GA-2013-606839, part of the 7th Framework Programme, Marie Curie actions. Thanks to A Lewis for his critical review and comments. Gratitude and thanks to D Cambell, J Baldwin, and K Summerhays for their guidance and provision of the PUNDITCMM™ software [71] used for CMM uncertainties studies. Special thanks as well to K Doytchinov for his professional feedback, guidance and support.

## ORCID iDs

I Doytchinov  <https://orcid.org/0000-0003-3871-0377>

## References

- [1] CLIC (Collaboration) 2012 *A Multi-TeV Linear Collider Based on CLIC Technology Conceptual Design Report* (Geneva: CERN)
- [2] Mainaud Durand H and Touze T 2006 The active pre-alignment of the CLIC components *9th Int. Workshop On Accelerator Alignment (Stanford, USA)*
- [3] Mainaud Durand H 2016 Fiducialisation and initial alignment of the CLIC components within a micrometric accuracy *14th Int. Workshop on Accelerator Alignment*
- [4] Hexagon A B 2017 *Leitz PMM-C Manufacturer Website and Descriptions* <http://hexagonmi.com/products/coordinate-measuring-machines/bridge-cmms/leitz-pmmc> (Accessed: September 2016)
- [5] BIPM 2006 *International System of Units (SI)*
- [6] Bottura L, Buzio M, Pauletta S and Smirnov N 2006 Measurement of magnetic axis in accelerator magnets: critical comparison of methods and instruments *IEEE Instrumentation and Measurement Technology Conf. Proc.* pp 765–70
- [7] Arpaia P, Caiazza D, Petrone C and Russenschuck S 2015 Performance of the stretched and vibrating wire techniques and correction of background fields in locating quadrupole magnetic axes *XXI IMEKO World Congress 'Measurement in Research and Industry'*
- [8] Mainaud Durand H et al 2017 Main achievements of the PACMAN project for the alignment at micrometric scale of accelerator components *IPAC 2017*
- [9] Sanz C, Cherif A, Mainaud Durand H, Schneider J, Steffens N, Morantz P and Shore P 2015 New potential for the Leitz Infinity coordinate measuring machine *EUSPEN Int. Conf. & Exhibition*
- [10] Turner S and (CAS-CERN Accelerator School) 1998 *Measurement and Alignment of Accelerator and Detector Magnets* (Geneva: CERN)
- [11] Trbojevic D, Jain A, Tepikian S, Grandinetti R, Ganetis G, Wei J and Karl F 1998 *Alignment of the High Beta Magnets in the RHIC Interaction Regions (Vancouver, Canada)* (Institute of Electrical and Electronics Engineers Inc.)
- [12] Wolf Z, Ruland R, Dix B and Arnett D 2005 Alignment tools used to locate a wire and a laser beam in the VISA undulator project *IWAA*
- [13] Egawa K, Masuzawa M, Ibaraki J and (KEK) 1998 Preliminary results of the KEKB quadrupole magnet measurements *EPAC*
- [14] Vasserman I 2000 *Quadrupole Magnetic Center Definition Using the Hall Probe Measurement Technique*
- [15] Wolf Z, Kaplunenko V, Levashov Y and Weidemann A 2007 LCLS undulator tuning and fiducialization 2007 *IEEE Particle Accelerator Conf. (PAC)* pp 1320–2
- [16] Slac Z W 2005 A Vibrating Wire System for Quadrupole Fiducialization *LCLS Technical Notes* Stanford, CA
- [17] Chida Y, Ohnishi J and Matsui S 1995 Laser and CCD camera system for magnet alignment on girder in the SPring-8 storage ring *eConf.* vol C951114 pp 194–200
- [18] Fischer G E, Bressler V E, Cobb J K, Jensen D R, Ruland R E, Walz H V and Williams S H 1992 Precision Fiducialization of Transport Components *Proceedings EPAC (Berlin)*
- [19] Farkhondeh M, Holmberg S P, Sapp W W and Zumbro J D 1991 Fiducialization of magnets for the MIT-bates SHR *Particle Accelerator Conf.* pp 634–6
- [20] Di Marco J 2005 LHC IR quadrupole alignment experience at Fermilab *14th Int. Magnetic Measurement Workshop (CERN)*
- [21] Dupont M, Missiaen D and Winkes P 2004 The laser tracker: a major tool for the metrology of the LHC (Geneva: CERN) pp 4–7
- [22] Pérez J G, Galbraith P, Buzio M, Charrondiere C, Coccoli M, Laface E, Pauletta S and Ruccio A 2005 Axis measurement with AC mole: geometric and magnetic calibration **2709**
- [23] Temnykh A 2005 Magnetic survey of the CESR interaction region quadrupole magnets using vibrating wire technique *14th Int. Magnetic Measurement Workshop (CERN)*
- [24] Temnykh A 2005 Application of the vibrating wire technique for solenoid magnetic center finding *14th Int. Magnetic Measurement Workshop (CERN)*
- [25] Loulergue A 2005 Status of the SOLEIL booster synchrotron *Proc. IEEE Particle Accelerator Conf.* vol 2005 pp 2155–7
- [26] Zangrando D and Walker R P 1993 Magnetic measurement and alignment of the ELETTRA storage ring quadrupole, sextupole and steerer magnets *Conf. Proc.* vol C930517 pp 2844–6
- [27] Pagano O, Rohmig P, Walckiers L and Wyss C 1984 A highly automated measuring system for the LEP magnetic lenses *Le J. Phys. Colloq.* **45** C1-949–52
- [28] Van Gestel N 2011 Determining Measurement Uncertainties of Feature Measurements on CMMs *PhD Thesis* Leuven University
- [29] Doytchinov I 2017 Alignment measurement uncertainties for large assemblies via probabilistic modeling techniques *PhD Thesis* Cranfield University
- [30] Wilhelm R G, Hocken R and Schwenke H 2001 Task-specific uncertainty in coordinate measurement *CIRP Ann.—Manuf. Technol.* **50** 553–63
- [31] JCGM 2008 *Evaluation of Measurement data—Guide to Uncertainty in Measurement* (Paris: BIPM)
- [32] Leão R, Baldob C, Reisc M, Trabancod J L A, Rodrigues F and Neuenschwander R 2016 Magnet alignment on a common girder: development of a length artefact for measurement accuracy improvement *J. Int. Soc. Precis. Eng. Nanotechnol.*
- [33] JCGM 2008 *Evaluation of Measurement Data—Supplement 1 to the 'Guide to the Expression of Uncertainty in Measurement'—Propagation of Distributions using a Monte Carlo Method* (Paris: BIPM)
- [34] Trenk M, Franke M and Schwenke H 2004 The 'Virtual CMM' a software tool for uncertainty evaluation—practical application in an accredited calibration lab *ASPE Proc.: Uncertainty Analysis in Measurement and Design* p 6
- [35] Phillips S D et al 1997 The calculation of CMM Measurement uncertainty via the method of simulation by constraints *Proc. 12th Annual Meeting of the American Society for Precision Engineering* pp 443–6
- [36] Schwenke H, Knapp W, Haitjema H, Weckenmann A, Schmitt R and Delbressine F 2008 Geometric error measurement and compensation of machines – an update *CIRP Ann.—Manuf. Technol.* **57** 660–75
- [37] Trapet E and Wäldele F 1991 A reference object based method to determine the parametric error components of coordinate measuring machines and machine tools *Measurement* **9** 17–22
- [38] ISO draft/FDIS 2010 *Geometrical Product Specifications (GPS)—Acceptance and Reverification Tests for Coordinate Measuring Machines (CMM)—Part 5* (Geneva: International Organization for Standardization)
- [39] Phillips S, Borchardt B, Abackerli A J, Shakarji C and Sawyer D 2003 The validation of CMM task specific measurement uncertainty software *Proc. ASPE 2003 Summer tropical Meeting 'Coordinate Measuring Machines'*
- [40] METROSAGE 2009 PUNDITCMM:: metrosage <http://metrosage.com/punditcmm.html> (Accessed: 12 June 2017)
- [41] Kucuk S and Bingul Z 2006 Robot kinematics: forward and inverse kinematics *Industrial Robotics: Theory, Modelling and Control* (Mammenford: Pro Literatur Verlag) in German
- [42] Summerhays K, Baldwin J, Campbell D and Henke R 2004 Application of simulation software to coordinate

- measurement uncertainty evaluation *ASPE Uncertainty Analysis in Measurement and Design* (2004)
- [43] Weckenmann A, Knauer M and Kunzmann H 1998 The influence of measurement strategy on the uncertainty of CMM measurements *CIRP Ann.—Manuf. Technol.* **47** 451–4
- [44] Ramesh R, Mannan M and Poo A 2000 Error compensation in machine tools—a review *Int. J. Mach. Tools Manuf.* **40** 1257–84
- [45] Phillips S D, Borchardt B, Estler W and Buttress J 1998 The estimation of measurement uncertainty of small circular features measured by coordinate measuring machines *Precis. Eng.* **22** 87–97
- [46] ISO/TS 23165 2006 *Geometrical Product Specifications (GPS)—Guidelines for the Evaluation of Coordinate Measuring Machine (CMM) Test Uncertainty* (Geneva: International Organization for Standardization)
- [47] ISO 14253-1 2013 *Geometrical Product Specifications (GPS)—Inspection by Measurement of Workpieces and Measuring Equipment—Part 1: Decision Rules for Proving Conformity or Nonconformity with Specifications* (Geneva: International Organization for Standardization)
- [48] Bryan J, Pearson J, Brewer W and McClure E 1965 Thermal effects in dimensional metrology *Mech. Eng.* **87** 70
- [49] Bryan J B 1967 International status of thermal error research *CIRP Manuf. Technol.* **39** 645–56
- [50] Weck M, McKeown P, Bonse R and Herbst U 1995 Reduction and compensation of thermal errors in machine tools *CIRP Ann.—Manuf. Technol.*
- [51] Doiron T D 2001 *Temperature and Dimensional Measurement* <http://emtoolbox.nist.gov/Temperature/Temperature and Dimensional Measurement.pdf> (Accessed: 13 June 2017)
- [52] Bryan J B and Doiron T 2011 *Temperature fundamentals Coordinate Measuring Machines and Systems* 2nd edn (Boca Raton, FL: CRC Press) pp 273–303
- [53] Trapet E 2010 Temperature effects in dimensional metrology; influences of temperature on the accuracy and how to cope with them *CIMI* pp 1–5
- [54] ISO 1101 2017 *Geometrical Product Specifications (GPS)—Geometrical Tolerancing—Tolerances of Form, Orientation, Location and Run-out* (Geneva: International Organization for Standardization)
- [55] NIST 2014 *SOP No. 29 Standard Operating Procedure for the Assignment of Uncertainty*
- [56] Morse E and Bhamidi K 2003 *Uncertainty of Measurements Using Multisensor CMMs* (Raleigh, NC: ASPE Annual Publications)
- [57] Bhamidi K and Morse E P 2004 *Performance Testing of Multisensor CMMs Based on Single Artifact Measurement* (Raleigh, NC: ASPE Annual Publications)
- [58] ISO 15530-4 2008 *Geometrical Product Specifications (GPS)—Coordinate Measuring Machines (CMM): Technique for Determining the Uncertainty of Measurement—Part 4: Evaluating Task-Specific Measurement Uncertainty Using Simulation* (Geneva: International Organization for Standardization)
- [59] ISO 10360-9 2013 *Geometrical Product Specifications (GPS)—Acceptance and Reverification Tests for Coordinate Measuring Systems (CMS)—Part 9: CMMs with Multiple Probing Systems* (Geneva: International Organization for Standardization)
- [60] ISO 14253-2 2011 *Geometrical Product Specifications (GPS)—Inspection by Measurement of Workpieces and Measuring Equipment—Part 2: Guidance for the Estimation of Uncertainty in GPS Measurement in Calibration of Measuring Equipment* (Geneva: International Organization for Standardization)
- [61] ISO 5459 2011 *Geometrical Product Specifications (GPS)—Geometrical Tolerancing—Datums and datum Systems* (Geneva: International Organization for Standardization)
- [62] Summerhays K, Baldwin J, Campbell D and Henke R 2004 Application of simulation software to coordinate measurement uncertainty evaluation *ASPE Proc., Uncertainty Analysis in Measurement and Design*
- [63] Carl Zeiss AG 2017 *ZEISS PRISMO CMM—Manufacturers* <https://zeiss.com/metrology/products/systems/bridge-type-cmms/prismo-navigator.html> (Accessed: 20 June 2017)
- [64] Trapet E 2015 *Inter-Laboratory Tetrahedron Comparison and Artifact Study* (<https://doi.org/10.5281/ZENODO.842757>)
- [65] Trapet E 2017 *Trapet Precision Engineering* <http://trapet.de/> (Accessed: 12 June 2017)
- [66] Zhang X 2013 Metrology-based process modelling framework for digital and physical measurement environments integration *PhD Thesis* University of Bath
- [67] Caiazza D 2017 Metrological performance enhancement of wire methods for magnetic field measurement in particle accelerators *PhD Thesis* University of Sannio
- [68] ISO 15530-1 2013 *Technique for Determining the Uncertainty of Measurement Part 1: Overview and Metrological Characteristics* (Geneva: International Organization for Standardization)
- [69] Etalon A G 2017 *LaserTRACER-NG* <http://etalon-ag.com/en/products/lasertracer/> (Accessed: 03 November 2017)
- [70] CERN 2017 *PACMAN Innovative Doctoral Program* <https://pacman.web.cern.ch/> (Accessed: 31 July 2017)
- [71] Metrosage LLC *Metrosage* <http://metrosage.com/> (Accessed: 20 October 2017)